Optimisation of Process Parameters of FSW welding of HE-30 Aluminium alloy

M. Venkata Ramana[1], *Madarapu* Anjaiah[2], *R*. Sudarshan[3], J*alumedi* Babu[4], *A*. Jeevansathwik[1] and *N*. Yakub[1]

[1] CVR College of Engineering, Mangalpalli, Ibrahimpatnam (Mandal), Hyderabad,501510, India.
[2]Department of Mechanical Engineering, Guru Nanak Institutions Technical Campus, Ibrahimpatnam, Hyderabad, 501506 Telangana, India.
[3]Geethanjali College of Engineering and Technology, Hyderabad, India.
[4]IMPACT College of Engineering and Applied Sciences, Sahakar Nagar South, Kodigenahali Bangalore,560092, India.

Abstract. HE-30 aluminum alloy has been extensively used in the aerospace, automobile and marine industries. This paper attempted process parameter optimisation of a welded joint of HE-30 aluminium alloy joined through FSW. Three-level factors, namely rotational speed of tool, traverse speed of tool, and tool geometry, are taken into account. Responses are ultimate tensile strength, yield strength and percentage of elongation. ANOVA is performed. It has been observed that the type of tool used has a pronounced effect, with the threaded type yielding the best results.

1. Introduction

Friction-stir welding, with a rotating tool made of hard materials like hot work tool steel, is more advantageous than fusion welding methods. The type and shape of the tool play a predominant role in dictating the quality of the FSW joint [1]. Frictional heat created by the tool due to its rotation and axial pressure on workpiece material is responsible for the preparation of a good quality welded joint. The tool employed for the FSW process should maintain its toughness while operating at high temperatures of the FSW process that exhibit sufficient resistance to pressures encountered during plunging and advanced phases. Simultaneously, the tool should have sufficient capacity to send out the generated heat. A variety of tool geometries are employed based on the type of workpiece material and its thickness. Tools with double shoulders are made to prepare a good FSW joint for thicker workpieces [2]. Generally, in the FSW process, the maximum temperatures generated due to friction are in the order of 80 to 90% of the melting temperature [3]. The pin provided at the end of the tool plays a vital role in the alternation of microstructures of workpieces during the FSW process [4, 5]. A positive effect of pin eccentricity on the quality of the joint is reported [6]. The quality of an FSW-welded joint depends upon tool dwell time, rotational speed, tool traverse speed, and axial pressure [7]. By virtue of its ability to bond the material due to friction and consequent intense heat, FSW finds numerous applications in the welding of aluminium alloys, copper alloys, and steels [8]. Evolution of the FSW technique made possible the joining of different materials with substantial differences in welding properties, leading to lightweight multi-material assemblies. In the FSW process, it is possible to reduce the heat-affected zone compared to the traditional welding method. Grain growth is reported in the HAZ while the weld region experiences reduced grain sizes [9]. Control of force and temperature monitoring in the FSW process is important. Fluctuations in axial forces and temperatures employed during the FSW process are observed. It is attempted to quantify the influence of various factors of the FSW welding process on temperature variations. Employing higher speeds of tool rotation and lower tool traverse speeds promotes a significant rise in temperature at the welding line. It is observed that compatibility of workpiece and tool materials, their thermal properties, and material flow behavior under heat play an important role in deciding the quality of the FSW joint, which can be resolved through appropriate material combination and FSW joint design. [10]. FSW joints yield high-strength joints whose strength is almost equal to base metal. Especially, the FSW joint is free of welding defects related to fusion that contribute to higher joint strength. The quality of FSW joints depends on parameters, speed of welding, tilt angle of tool, and axial pressure, as reported in [11]. Optimization of these parameters enhances FSW joint strength. Literature reveals articles on the application of optimization techniques for manufacturing processes [12-13]. The structural integrity of an FSW joint depends on tensile strength. Investigations were done on both FEA works and experimental investigations on the tensile behavior of FSW joints, which are reported [14-16]. HE-30 aluminum alloy is a heat-treatable Al-Mg-Si alloy that is widely used in the automobile industry, aerospace, and marine applications. HE-30 alloy has excellent corrosion resistance and weldability and is lighter in weight. This investigation attempts FSW process parameter optimization of FSW joints made of HE-30 aluminum alloy. Process parameters taken into account are rotational speed of tool, traverse speed of tool, and geometry of tool with an objective of maximizing the strength of joint.

2. Material

HE-30 Aluminium alloy is the workpiece material. Aluminium HE 30 is primarily composed of aluminium, with significant additions of magnesium and silicon that enhance its strength by forming Mg_2Si precipitates and manganese, which controls grain structure and boosts mechanical strength. The composition of material used in the study is given in the table. 1.

Table.1. HE-30 Aluminium alloy composition

Element	Mg	Si	Mn	Others
Percentage	0.6	1	0.75	< 0.5

3. Experimentation

3.1 Process Parameters

Three-level factors, namely rotational speed of tool, traverse speed of tool, and tool geometry, are taken into account.

Rotational speed of tool: The problem with the too-low tool rotational speed is it leads to insufficient plastic flow and consequent defects and inferior strength of the joint. On the other hand, higher tool rotational speeds lead to excessive heat, leading to excessive grain coarsening of precipitates and excessive softening of HAZ, leading to inferior joint strength. Generally, the range for tool rotational speed is 800 to 1600 rpm. In this study, rotational speeds of the tool were taken from the 800 to 1600 rpm range.

Traverse speed of tool: Traverse speed of tool influences heat input & welding zone cooling rate. Lower tool traverse speed causes softening of HAZ and excessive grain coarsening may lead to inferior yield strength while higher traverse speed causes insufficient plasticised weld zone leading to formation of weld defects. Three levels of tool traverse speed are considered. Tool geometry: The proper shoulder of the tool is necessary to inhibit expulsion of plasticized material. The pin indicates the degree of stirring during the welding zone. Tool geometry influences the forging pressure, heat generation, plasticized material flow path, and stirring of the weld zone. Three geometries, namely cylindrical, threaded, and conical pins, are considered. Different tool profiles used in the experiment are shown in Fig. 1. Process parameters and levels are tabulated in the table. 2.

Table.2. Parameters and levels.

Parameter	Unit	Level 1	Level 2	Level 3
Rotational Speed of tool	RPM	900	1200	1400
Traverse Speed of tool	M mm/minute	30	60	90
Tool Geometry	-	Cylindrical	Threaded	Conical

Different types of tool profiles used in the study are given figure-1.

3.2 Experimental Design Matrix

To accommodate three factors at three levels Taguchi's L9 orthogonal array is chosen as experimental plan.

Responses:

Three responses, namely ultimate tensile strength, yield strength, and percentage of elongation, are considered. Ultimate tensile strength is the indication of the quality of an FSW joint, and hence the quality characteristic is "Higher the better." Yield strength is the indication of joint strength with sufficient ductility. The quality characteristic for yield strength is "higher the better." Percentage of elongation is another response. A higher percentage of elongation reflects better service performance, fatigue resistance, and equiaxed grains of the mixing zone. A smaller percentage of elongation is the indication of brittle fracture inclination with voids in the weld zone. The quality characteristic is "higher the better."

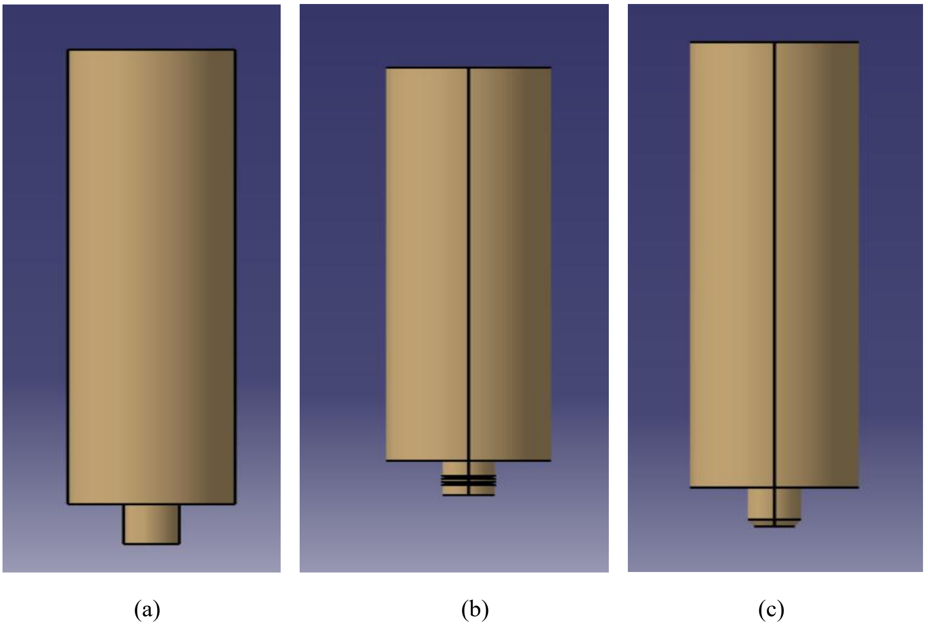

Fig.1. Different tool profiles used(a)Square pin (b) Threaded pin (c)Conical pin.

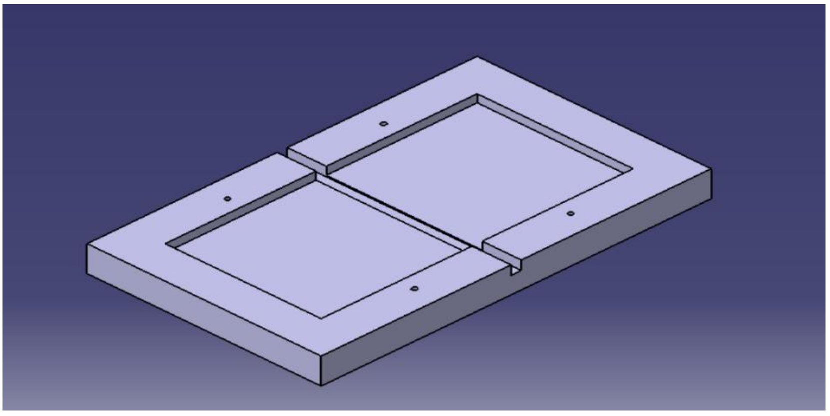

Fig. 2. Mould prepared to prepare proper FSW joint.

3.2 FSW joint preparation

As per the experimental plan, FSW joints are prepared using a CNC milling machine. A CNC machine enables the control of the spindle speed, feed rate and cutting depth, which results in high accuracy and a superior finish. A mould was prepared as shown in Fig. 2, which ensures the workpiece's rigidity during FSW joint preparation. Mould is shown in Fig. 2. Workpieces with the mould assembly are shown in Fig. 3(a). Fig. 3(b) depicts FSW joint preparation. A prepared FSW joint is given in Fig.4.

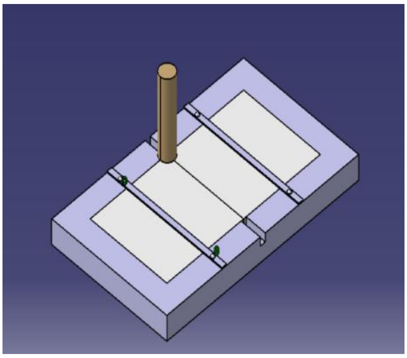

Fig.3(a). Work piece and Mould assembly.

Fig.3(b). FSW joint preparation.

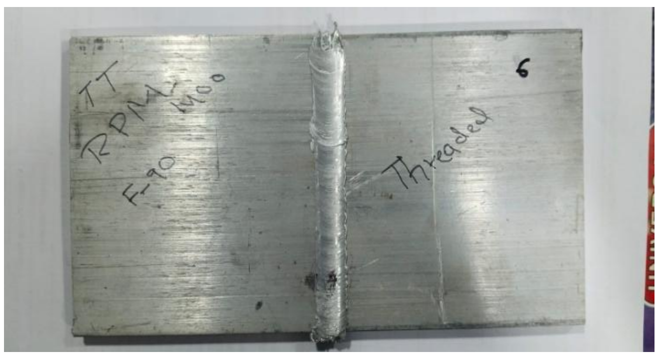

Fig. 4. FSW joint.

3.3 Tensile Testing

Tensile testing was conducted as per ASTM D8 standards, and the tensile testing sample sketch is shown in Fig. 5(a). Tensile test samples are cut from the prepared FSW joints across the joint, with centre of the FSW joint being the centre of the tensile testing specimen. Tensile test samples cut from the FSW joint are shown in Fig. 5(b).

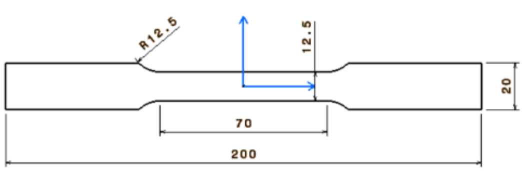

Fig. 5(a). Standard tensile test specimen.

Fig.5(b). Prepared Tensile test samples.

4. Results

All the tensile test samples prepared were subjected to tensile testing. Each experiment is replicated thrice, and S/N values are computed. The experimental plan with actual level values of parameters along with actual S/N ratio values of UTS, strength at yield point, and elongation percentage is given in Table 3. Stress-strain diagrams of samples prepared from each experimental trial combination are given in Fig. 6. S /N analysis was made. Based on S/N analysis, the response graphs are drawn to identify optimum levels. Response graphs are shown in Fig. 7. Microstructures of FSW joints at the base metal, HAZ, and weld zone are given in Fig. 8.

Table-3. Experimental Plan with actual values and S/N ratios of UTS, YS and % of elongation.

Experiment Number	**Rotational speed of tool (rpm)**	**Traverse Speed of Tool(mm/minute)**	**Geometry of Tool**	**UTS (MPa)**	**Strength at yield point (MPa)**	**Percentage elongation**	**Ultimate UTS (S/N ratio)**	**Strength at yield point (S/N ratio)**	**Percentage elongation (S/N ratio)**
1	900	30	Cylindrical	14.78	10.82	1.2444	23.3935	20.6845	1.89920
2	900	60	Threaded	69.28	62.5	2.4	36.8122	35.9176	7.60422
3	900	90	Conical	31.46	26.98	0.88	29.9552	28.6208	-1.11035
4	1200	30	Threaded	75.684	61.659	2.60	37.5801	35.7999	8.29947
5	1200	60	Conical	41.64	38.4	1.15	32.3902	31.6866	1.21396
6	1200	90	Cylindrical	21.46	19.45	1.2	26.6326	25.7784	1.58362
7	1400	30	Conical)	31.99	27.76	0.78	30.1003	28.8684	-2.15811
8	1400	60	Cylindrical	18.86	15.48	1.18	25.5108	23.7954	1.43764
9	1400	90	Threaded)	74.32	68.26	2.58	37.4221	36.6833	8.23239

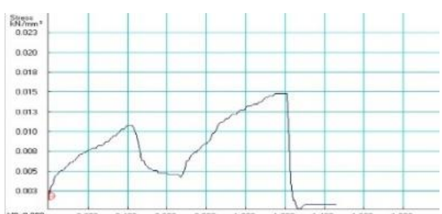

(a)

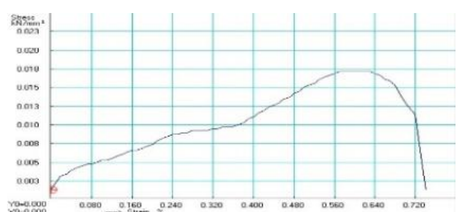

(b)

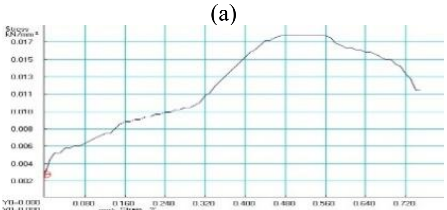

(c)

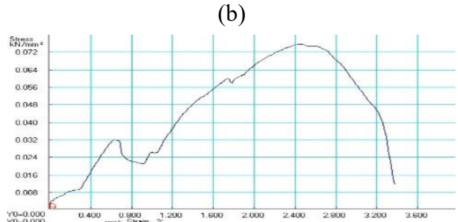

(d)

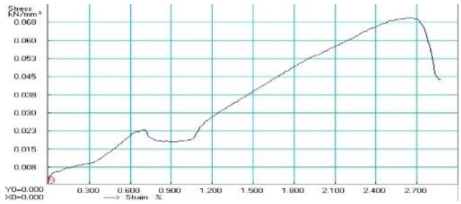

(e)

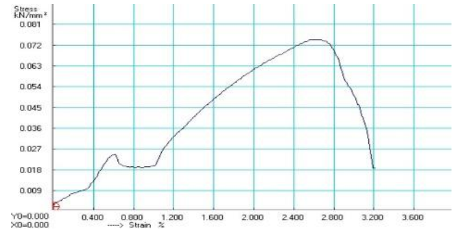

(f)

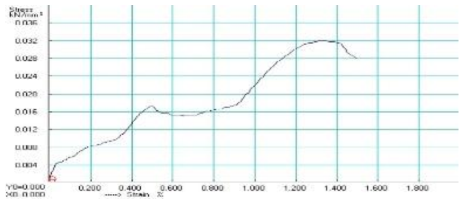

(g)

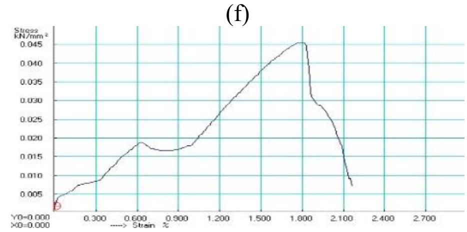

(h)

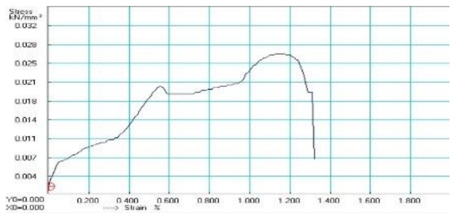

(i)

Fig.6. Stress Strain Diagrams of samples made from FSW joint with(a) first experimental trial (b) Second experimental Trial (c) Third Experimental Trial (d) Fourth Experimental Trial (e)Fifth Experimental Trial (f) Sixth etc..

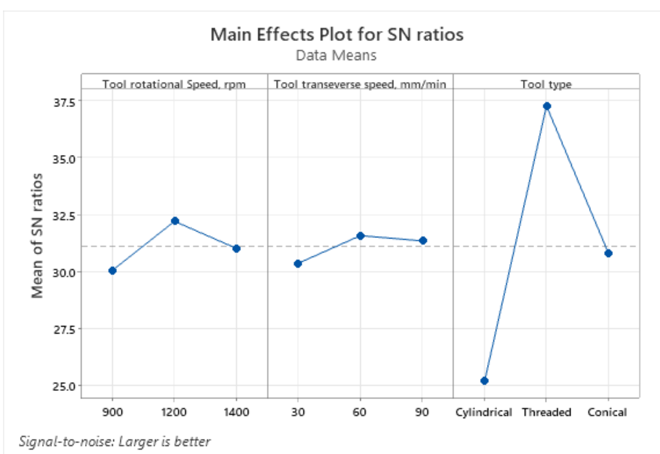

Fig.7(a). Response Graph for Ultimate Tensile Strength.

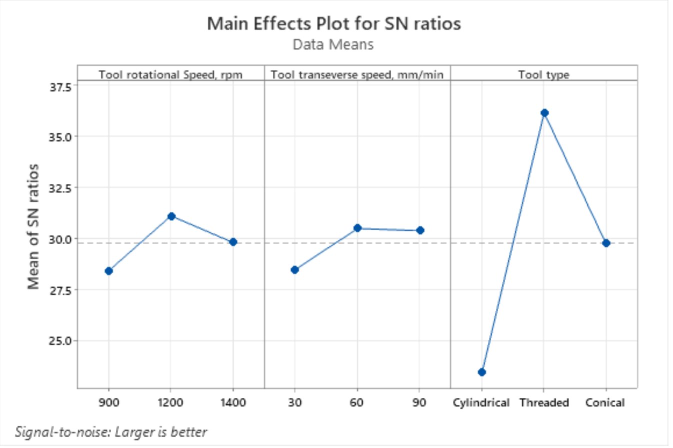

Fig. 7(b). Response Graph for Yield Strength.

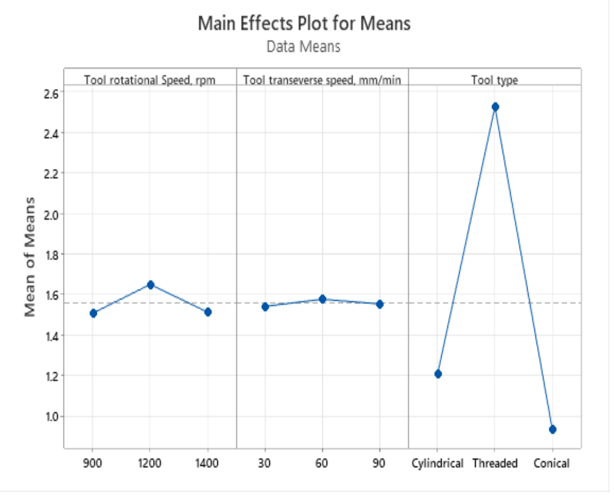

Fig. 7(c). Response Graph for % of elongation.

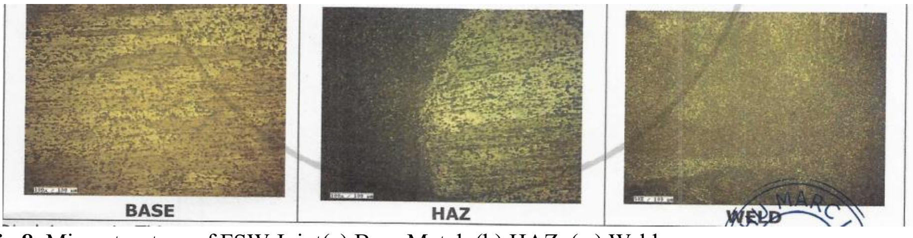

Fig.8. Microstructure of FSW Joint(a) Base Metal (b) HAZ (c) Weld zone.

4.1 Optimum Condition

From the response graph of UTS (Fig. 7-a), yield strength (Fig. 7-b), and percentage of elongation (Fig. 7-c), the optimum level of process parameters is decided and tabulated in Table 4. Analysis of variance is conducted to discriminate the significant and insignificant factors. In all three cases it was observed that the type of tool is the most significant factor, especially since the threaded type of tool yields the best results among the considered tool types.

Table.4. Optimum Condition.

S. No	Response Characteristic	Process Parameters		
		Rotational speed of tool(rpm)	Traverse speed of tool(mm/min)	Tool Geometry
1	Ultimate Tensile Strength	1200	60	Threaded
2	Yield Strength	1200	60	Threaded
3	Percentage of elongation	1200	60	Threaded

5. Conclusion

In this study, process parameters for FSW joints of aluminium alloy HE-30 are optimised for better ultimate tensile strength and elongation percentage. Tool geometry significantly affects responses. It was found that a tool rotational speed of 1200 rpm and a 30 mm/minute tool traverse speed with a threaded-type tool yielded the best results.

.

References

1. S. Hassanifard, A. Hashemi, A. Varvani-Farahani, M. Ghiasvand, The effect of the friction stir welding tool shape on tensile properties of welded Al 6061-T6 joints. Mater. Today Commun. 31, 103457 (2022). https://doi.org/10.1016/j.mtcomm.2022.103457
2. K. Fuse, V. Badheka, Bobbin tool friction stir welding: A review. Sci. Technol. Weld. Join. 24, 277–304 (2019). https://doi.org/10.1080/13621718.2018.1553655
3. Z. Ma, A. Feng, D. Chen, J. Shen, Recent advances in friction stir welding/processing of aluminum alloys: Microstructural evolution and mechanical properties. Crit. Rev. Solid State Mater. Sci. 43, 269–333 (2018). https://doi.org/10.1080/10408436.2017.1358145
4. Y. Li, D. Sun, W. Gong, Effect of tool rotational speed on the microstructure and mechanical properties of bobbin tool friction stir welded 6082-T6 aluminum alloy. Metals 9, 894 (2019). https://doi.org/10.3390/met9080894
5. R.S. Mishra, Z.Y. Ma, Friction stir welding and processing. Mater. Sci. Eng. R Rep. 50, 1–78 (2005). https://doi.org/10.1016/j.mser.2005.07.001
6. W. Hou, Y. Ding, G. Huang, N. Huda, L.H.A. Shah, Z. Piao, Y. Shen, Z. Shen, A. Gerlich, The role of pin eccentricity in friction stir welding of Al-Mg-Si alloy sheets: Microstructural evolution and mechanical properties. Int. J. Adv. Manuf. Technol. 121, 7661–7675 (2022).
7. T. Ding, H.G. Yan, J.H. Chen, W.J. Xia, B. Su, Effect of welding speed on microstructure and mechanical properties of Al-Mg-Mn-Zr-Ti alloy sheet during friction stir welding. Trans. Nonferrous Met. Soc. China 31, 3626–3642 (2021).
8. G. Nagesh, N. Rao, K. Kanishk, K.M. Anurag, N. Abhinav, Investigation of mechanical properties on non-ferrous alloys of copper and brass joints made by friction stir welding. IOP Conf. Ser. Mater. Sci. Eng. 1057, 012062 (2021).

9. N.T. Moghaddam, A. Rabiezadeh, A. Khosravifard, L. Ghalandari, Self-reacting friction stir welding of Al–Zn–Mg aluminum alloy. Arab. J. Sci. Eng. 47, 9085–9098 (2022).
10. S. Kilic, F. Ozturk, M.F. Demirdogen, A comprehensive literature review on friction stir welding: Process parameters, joint integrity, and mechanical properties. J. Eng. Res. 13, 122–130 (2025).
11. B. Abnar, S. Gashtiazar, M. Javidani, Friction stir welding of non-heat treatable Al alloys: Challenges and improvement opportunities. Crystals 13, 576 (2023). https://doi.org/10.3390/cryst13040576
12. A. Madarapu, J. Babu, M. Venkata Ramana, Optimisation of pressure and depth of forming for box shaped super plastic forming of AZ31B magnesium alloy. Mater. Today Proc. 58(1), 205–211 (2022). https://doi.org/10.1016/j.matpr.2022.01.445
13. J. Babu, A. Madarapu, T. Sunny, M. Venkata Ramana, Multi characteristic optimisation of high speed machining of GFRP laminate by hybrid Taguchi desirability approach. Mater. Today Proc. 58(1), 238–243 (2022). https://doi.org/10.1016/j.matpr.2022.02.097
14. K. Ramakanth, P. Yugandhar Babu, G. Venkata Jagadeesh, Subhashish Dey, G. Taraka Naga Veerendra, Prediction and optimization of process parameters of friction stir welded aluminum 6063 alloy, Journal of Alloys and Compounds Communications. 8,100105 (2025).
15. A. Kumar, P. Pankaj, P. Biswas, A.G. Rao, Finite element analysis and experimental investigation on effect of process parameters in plasma-assisted friction stir welding of low carbon steel. Trans. Indian Inst. Met. 75, 2559–2579 (2022).
16. B. Meyghani, M. Awang, S. Emamian, A comparative study of finite element analysis for friction stir welding application. ARPN J. Eng. Appl. Sci. 11, 12984–12989 (2016).